



Nonlinear current Controller for Enhancing Dynamic performance of Single Phase Grid Connected PV system

Ms. Ashwini A. Pakhale¹, Prof. A. D. Matre²

^{1,2}Electrical, GES's R.H. Sapat College of Engineering, Management Studies & Research,
Nashik, Pune University,(India)

ABSTRACT

This paper presents a new nonlinear current control scheme for a single-phase grid-connected photovoltaic (PV) system. partial feedback linearization is used for designing the controller, which linearizes the system partially and enables the controller design scheme for reduced-order PV systems. The reference current is calculated from the maximum power point tracking system. The proposed current control approach introduces the internal dynamics and the stability of the internal dynamics is a key requirement for the implementation of the controller to analyze the stability of internal dynamics of a PV system. Based on the tracking of grid current to the reference current, the performance of the controller is evaluated by considering the changes in environmental conditions. A large system similar to a practical system is simulated under different operating conditions such as changes in atmospheric conditions and faults on various parts of the system and compared with hysteresis controllers, which ensures the suitability of the proposed controller in a real system.

Keywords- *Current controller, grid connected photovoltaic (PV) system, maximum power point tracking, partial feedback linearizing controller.*

I. INTRODUCTION

In recent years, demand for energy has increased. In the world energy consumption is projected to grow by 49 percent from 2007 to 2030. This is because the development of countries is dependent on energy. In the field of power sector one of the major concerns in these days is day-by-day increase in power demand. But, the quantity and availability of conventional energy sources are not enough to meet up the current day's power demand. While thinking about the future availability of conventional sources of power generation, it becomes very important that the renewable energy sources must be utilized along with source of conventional energy generation systems to fulfill the requirement of the energy demand. In order to overcome current day's energy crisis, one renewable method is to extract power from the incoming sun radiation called Solar Energy, which is globally free for everyone. Solar radiation is widely available on the surface of earth as well as in space, so that we can harvest it and convert it into other form of energy and properly utilize it efficiently. Power generating unit may feed power into the grid or it may be used in isolated systems. Utility location, load center, available grid connectivity decides its energy usage. Thus, where the availability of grids connection is very difficult or costly, the solar energy can supply power to those areas. The most important two advantages of solar power are that its fuel cost is absolutely zero and solar power generation during its operation does not produce any greenhouse gases. Easy carry-in of the power generating unit is another advantage that is we can use it whenever wherever small power generation is required. In the last few years the power conversion mechanisms for solar



energy has been significantly reduced to compact size. The new researches in the field of power electronics and material science have greatly helped engineers to develop such systems. So that very small but effective and powerful systems that have capability to meet high electric power demand has been developed. For every country, day by day power density demand is increasing. Photovoltaic power generation is capable of mitigating voltage fluctuation very effectively by setting the system for the use of multiple input and converter units. But in solar power generation system, due to its high installation cost and the low efficiency of the solar cells, this power generating systems can hardly participate in the competitive power markets as a main renewable source of power generation.

The inclusion of proper controllers with a grid-connected PV system maintains the stable operation under disturbances such as changes in atmospheric conditions, changes in load demands, or an external fault within the system. This can be performed by regulating the switching signal of the inverter, i.e., if a proper controller is applied through the inverter switches, the desired performance can be achieved. Normally, maximum power point tracking (MPPT) techniques are employed to perform this task and there is extensive literature on MPPT techniques in [4]–[6]. The perturb and observe (PO) [7] and incremental conductance methods are commonly used techniques in the area of PV systems. In the PO method, the derivative of power (dp) and the derivative of voltage (dv) need to be measured to determine the movement of the operating point.[1] Current controllers are used for maintaining the stable operation of a grid-connected PV system as they can regulate the current to follow the reference current. There are various techniques to control the current such as proportional integral (PI) controllers, hysteresis controllers, predictive controllers, sliding-mode controllers, and so on. In [1] PI current control scheme is proposed to keep the output current sinusoidal and to have fast dynamic responses under rapidly changing atmospheric conditions. The difficulty of using a PI controller is the necessity of tuning the gain with changes in atmospheric conditions.

A comparative study on maximum power point tracking techniques for photovoltaic power systems. This researcher provides a comprehensive review of the maximum power point tracking (MPPT) techniques applied to photovoltaic (PV) power system available until January, 2012. A good number of publications report on different MPPT techniques for a PV system together with implementation. But, confusion lies while selecting a MPPT as every technique has its own merits and demerits. Hence, a proper review of these techniques is essential. Unfortunately, very few attempts have been made in this regard, excepting two latest reviews on MPPT. Since, MPPT is an essential part of a PV system, extensive research has been revealed in recent years in this field and many new techniques have been reported to the list since then. In this literature, a detailed description and then classification of the MPPT techniques have made based on features, such as number of control variables involved, types of control strategies employed, types of circuitry used suitably for PV system and practical/ commercial applications. This study is proposed to serve as a convenient reference for future MPPT users in PV systems. This review has included many recent hybrid MPPT techniques along with their benefits. Further, the review has also included MPPT techniques meant for mismatched conditions such as partial shading, non uniformity of PV panel temperatures, dust effects, damages of panel glass, etc. It has also given the idea of commercial products of MPPT techniques with the company names wherever possible. The review has discussed the efficiency calculation procedure of the developed MPPTs. This review is expected to

be a useful tool for not only the MPPT users but also the designers and commercial manufacturers of PV systems. [8]

In the previous literature the work is done on improvement of stability of single phase grid connected PV system by using PI controller. In this paper stability of single phase grid connected PV system is improved by designing partial Feedback Linearization Controller & compared with hysteresis controller under healthy atmospheric condition, fault conditions & environmental changes are considered.

The partial feedback linearization algebraically transforms nonlinear system dynamics into a partly linear one which is a reduced-order linear system and independent of operating points as the nonlinearities are canceled through nonlinear terms. The main advantage of partial feedback linearizing controllers is that the dynamics of the full model is not essential.

The aim of this paper is to design a new current controller through partial feedback linearization to control the current injected into the grid. The other novelty of this paper includes the stability of internal dynamics through the formulation Lyapunov function and the calculation of sinusoidal reference current which is essential for practical implementation. The performance of the proposed current control scheme is also investigated and compared with the hysteresis controller under healthy atmospheric condition, changes in atmospheric conditions & under fault condition.

II. SYSTEM DESCRIPTION

The overall system consists of solar panel that generates power according to the irradiation levels. The MPPT algorithm calculates the duty cycle for the converter corresponding to the maximum power point. The variation of the power and voltage of a solar panel is given in fig. 1. There will be one maximum power point for a particular irradiation [16]

Photovoltaic energy has increased interest in electrical power applications, since it is considered as a basically limitless and generally on hand energy resource. However, the output power induced in the photovoltaic modules depends on solar irradiance and temperature of the solar cells.

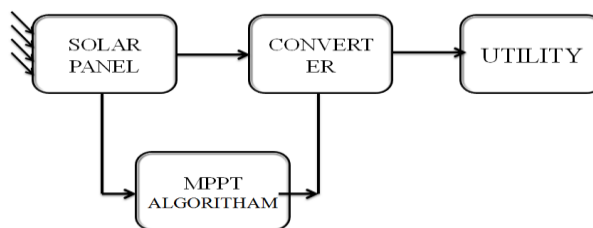


Fig. 1. Overall Systems

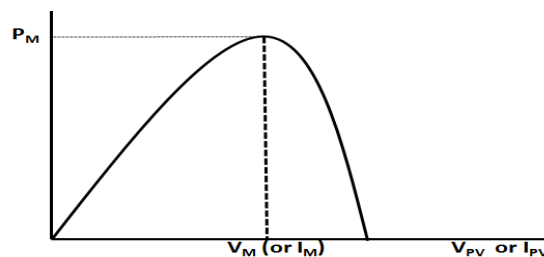


Fig. 2. Power–voltage characteristics of photovoltaic systems

This makes the extraction of maximum power a complex task. The efficiency of the PV generation depends on maximum power extraction of PV system. Therefore, to maximize the efficiency of the renewable energy system, it is necessary to track the maximum power point of the PV array. The PV array has a single in service point that can supply maximum power to the load. This point is called the maximum power point (MPP). The locus of this point has a nonlinear distinction with solar irradiance and the cell temperature. Thus, in order to operate the PV array at its MPP, the PV system must contain a maximum power point tracking (MPPT) controller. Many MPPT techniques have been reported in the literature.

III. PV SYSTEM MODEL

The schematic diagram of a single-phase grid-connected PV system, which is the main focus of this paper, is shown in Fig. 3. The PV system consists of a PV array, a dc-link capacitor C, a single-phase inverter, and a filter inductor connected to the grid with the voltage. In this project, the main target is to control the current injected into the grid by means of appropriate control signals through the switches of the inverter. The mathematical model of the system is presented in the following sections.

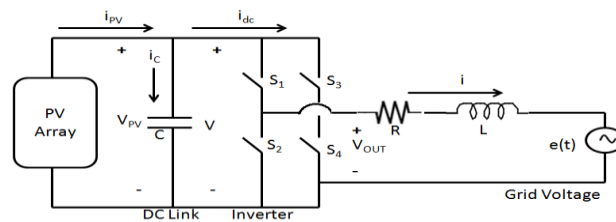


Fig. 3. Equivalent Circuit Diagram of Single-Phase Grid-Connected PV System

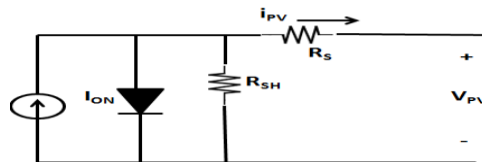


Fig. 4. Equivalent Circuit Diagram of PV Cell

3.1 PV Cell and Array Modeling

A PV cell is a simple p-n junction diode which converts the irradiation into electricity. Fig. 4. shows an equivalent circuit diagram of a PV cell which consists of a light generated current source I_L , a parallel diode, a shunt resistance R_{sh} , and a series resistance R_s . In Fig. 4. I_{ON} is the diode current which can be written as

$$I_{ON} = I_S [\exp[\alpha(V_{pv} + R_S i_{pv})]] - 1 \tag{1}$$

where α is a constant which is equal to q/AkT_C , $K=1.3807 \times 10^{-23} \text{ JK}^{-1}$ is Boltzmann's constant, $q=1.6022 \times 10^{-19} \text{ C}$ is the charge of electron, T_C is the cell's working temperature in kelvin, A is the p-n junction ideality factor whose value is between 1 and 5, I_S is the saturation current, and V_{PV} is the output voltage of the PV array which in this case is the voltage across C, i.e., V. Now, by applying Kirchhoff's current law (KCL) in Fig. 3, the output current (i_{pv}) generated by the PV cell can be written as

$$i_{pv} = I_L - I_s \left[\exp \left[\alpha (V_{pv} + R_s i_{pv}) \right] - 1 \right] - \frac{V_{pv} + R_s i_{pv}}{R_{sh}} \quad (2)$$

The light generated current I_L depends on the solar irradiation which can be related by the following equation:

$$I_L = [I_{sc} + K_i (T_c - T_{ref})] \frac{s}{1000} \quad (3)$$

where I_{sc} is the short-circuit current, s is the solar irradiation, K_i is the cell's short-circuit current coefficient, and T_{ref} is the reference temperature of the cell. The cell's saturation current I_s varies with the temperature according to the following equation [25]

$$I_s = I_{RS} \left[\frac{T_c}{T_{ref}} \right]^3 \exp \left[\frac{qE_g}{Ak} \left(\frac{1}{T_{ref}} - \frac{1}{T_c} \right) \right] \quad (4)$$

Where E_g is the band-gap energy of the semiconductor used in the cell and I_{RS} is the reverse saturation current of the cell at the reference temperature and solar irradiation. Since the output voltage of a PV cell is very low, a number of PV cells are connected together in series in order to obtain higher voltages. A number of PV cells are put together and encapsulated with glass, plastic, and other transparent materials to protect from a harsh environment to form a PV module. To obtain the required voltage and power, a number of modules are connected in parallel to form a PV array. Fig. 5 shows an electrical equivalent circuit diagram of a PV array, where N_s the number of cells in series is and N_p is the number of modules in parallel. In this case, the array current i_{pv} can be written as

$$i_{pv} = N_p I_L - N_p I_s \left[\exp \left[\alpha \left(\frac{V_{pv}}{N_s} + \frac{R_s i_{pv}}{N_p} \right) \right] - 1 \right] - \frac{N_p}{R_{sh}} \left(\frac{V_{pv}}{N_s} + \frac{R_s i_{pv}}{N_p} \right) \quad (5)$$

3.2 Single-Phase Grid-Connected PV System Modeling

In Fig. 3, the PV array represents the equivalent circuit diagram presented in Fig. 5, where v is the output of the dc link which is to be adjusted at a level through MPPT to make it suitable for the inverter, $S_1, S_2, S_3,$ and S_4 are the four switches of the inverter, R is the line resistance, L is the combination of filter and line inductance, i is the current injected into the grid, and $e(t) = V_m \sin \omega t$ is the grid voltage where V_m is the maximum value of the grid voltage, $\omega = 2\pi f$ is the angular frequency, and f is the grid frequency.

When S_1 and S_4 are ON, and S_2 and S_3 are OFF in Fig. 3, applying Kirchhoff's voltage law (KVL) and KCL, the following relationship can be obtained:

$$V = \frac{1}{C} (i_{pv} - i), \quad i = \frac{1}{L} (V - Ri - e) \quad (6)$$

When S_1 and S_4 are OFF, and S_2 and S_3 are ON in Fig. 3, again by applying KVL and KCL, the following relationship can be obtained

$$V = \frac{1}{C} (i_{pv} + i), \quad i = \frac{1}{L} (V - Ri - e) \quad (7)$$

Now by applying averaging technique, (6) and (7) can be written as

$$V = \frac{1}{C} (i_{pv} + i u(t)), \quad i = \frac{1}{L} (vu(t) - Ri - e) \quad (8)$$

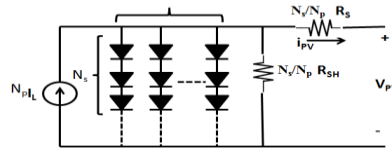


Fig. 5. Equivalent Circuit Diagram of PV Array

Equation (8) represents the complete mathematical model of a single-phase grid-connected PV system which is nonlinear due to the switching functions and diode current. In (8), u is the control input with a possible range of ± 1 and i is the output variable. Based on this model of PV systems, a control strategy is presented in Section III using a partial linearization control scheme.

IV. PARTIAL FEEDBACK LINEARIZATION AND PARTIAL LINEARIZABILITY OF PV SYSTEM

The mathematical model of a single-phase grid-connected PV system can be expressed as the general nonlinear system as follows:

$$\dot{x} = f(x) + g(x)u, \quad y = h(x) \tag{9}$$

Where

$$x = [v \quad i]^T, \quad f(x) = \begin{bmatrix} \frac{i_{pv}}{L} \\ \frac{c}{-R_i - c} \end{bmatrix}, \quad g(x) = \begin{bmatrix} -\frac{i}{L} \\ \frac{c}{L} \end{bmatrix}$$

And

$$y = i$$

The nonlinear system in (9) can be often linearized using feedback linearization. Consider the following nonlinear coordinate transformation:

$$Z = [h \quad L_f h(x) \quad \dots \quad L_f^{r-1} h(x)]^T \tag{10}$$

Where r is an integer and $L_f h(x) = \partial h / \partial x f(x)$ is the Lie derivative of $h(x)$ along $f(x)$. This transforms the nonlinear system (9) with the state vector z into a linear dynamic system with the state vector provided that the following conditions are satisfied for

$$n = r: L_g L_f^k h(x) = 0 \tag{11}$$

Where $k < r-1$ and

$$L_g L_f^k h(x) \neq 0 \tag{12}$$

Where $L_g L_f^k h(x)$ is the Lie derivative of $L_f h(x)$ along $g(x)$. The integer r is known as the relative degree of the system corresponding to the output function h . If these conditions are satisfied, a linear controller can be designed for the linearized system (13) which is also known as the exactly linearized system

$$\dot{z} = Az + Bv \tag{13}$$

Where A is the system matrix for the exactly linearized system, B is the input matrix for the exactly linearized system, and v is the new control input for the exactly linearized system. When $r < n$, we can perform only partial linearization and in this case, the transformed states z can be written as

$$Z = \phi(x) = [\tilde{z} \quad \hat{z}] \tag{14}$$

Where \hat{z} represents the states obtained from nonlinear coordinate transformation up to the order r and \hat{z} represents the states related to the remaining $n-r$ order. The dynamics of \hat{z} are called the internal dynamics whose stability need to be ensured before designing the linear controller for the following partially linearized system (15):

$$\dot{\hat{z}} = \hat{A}\hat{z} + \hat{B}\hat{v} \tag{15}$$

where \hat{A} is the system matrix for the partially linearized system, \hat{B} is the input matrix for the partially linearized system, and \hat{v} is the new control input for the partially linearized system.

The partial linearizability of the PV system represented in the form of (9) can be obtained by calculating the relative degree corresponding to the output function. The relative degree corresponding to $h(x) = i$ can be calculated as

$$L_g h(x) = L_g L_F^{1-1} h(x) = \frac{V_{PV}}{L} \tag{16}$$

Which indicates $r=1$ and $r < n$ as $n = 2$. Therefore, the system is partially linearized for the chosen output function. To implement the feedback linearizing control for this system, the partial feedback linearization approach needs to be used provided that the internal dynamics of the system is stable.

V. CURRENT CONTROLLER

5.1 Types of Current Controller

5.1.1 Hysteresis Current Controller

Hysteresis technique assumes instantaneous control between two limits, which require the offset signal, current or voltage, expected to follow the reference signal with some deviation imposed by the choice of hysteresis band width. Control scheme is illustrated by block diagram in Fig. 6. This control technique requires a deviation H of a reference signal which determines the upper and lower limits of the hysteresis band. Output signals are measured and compared with its reference value or the resulting error is applied to a controller with a changeover relay.

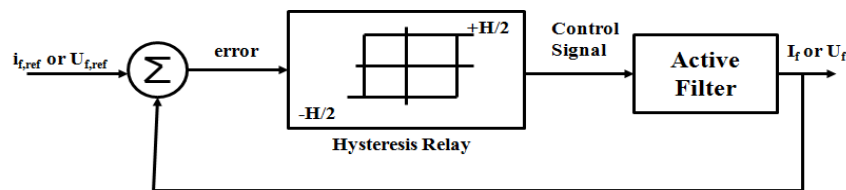


Fig. 6 Block Diagram of Hysteresis Control Technique: RBH-Changeover Hysteresis Relay.

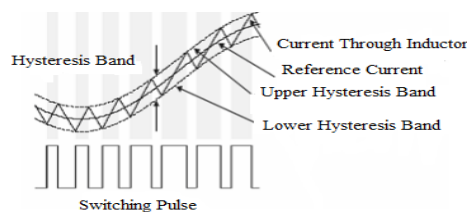


Fig. 7 Hysteresis Current Control

This generates control signals for power switching devices, when the lower (estimated reference - $H / 2$) or upper (estimated value of reference + $H / 2$) limit are exceeded. As long as the error is in the hysteresis band, power switching devices will not be switched. Switching occurs when the error is outside the hysteresis band.

Active filter is controlled so that the peak to peak value of the compensation signal, current or voltage is limited to specified hysteresis band H . The proposed scheme is implemented with hysteresis current controller with fixed band H . To obtain a compensated current with a current ripple as low as possible, the value of H should be small. This will lead to high switching frequencies and increasing the switching losses. Advantages of using the hysteresis current control are excellent dynamic performance and the ability to control the peak to peak value of current ripple in the specified hysteresis band. Implementation of this control technique is simple, which results from the controller structure in Fig. 7 However, the hysteresis control has several unsatisfactory features. The main disadvantage is that results in a variable switching frequency. On the other hand, irregular switching may affect the efficiency and reliability of active filter. [19].

5.1.2. Proportional Integral (PI) Controller

At present, the PI controller is most widely adopted in industrial application due to its simple structure, easy to design and low cost. Despite these advantages, the PI controller fails when the controlled object is highly nonlinear and uncertain. PI controller will eliminate forced oscillations and steady state error resulting in operation of on-off controller and P controller respectively. However, introducing integral mode has a negative effect on speed of the response and overall stability of the system. Thus, PI controller will not increase the speed of response. It can be expected since PI controller does not have means to predict what will happen with the error in near future. This problem can be solved by introducing derivative mode which has ability to predict what will happen with the error in near future and thus to decrease a reaction time of the controller. PI controllers are very often used in industry, especially when speed of the response is not an issue. A control without D mode is used when

- 1) Fast response of the system is not required
- 2) Large disturbances and noise are present during operation of the process
- 3) There is only one energy storage in process (capacitive or inductive)
- 4) There are large transport delays in the system.

Therefore, we would like to keep the advantages of the PI controller. This controller uses of the proportional term while the integral term is kept, unchanged.

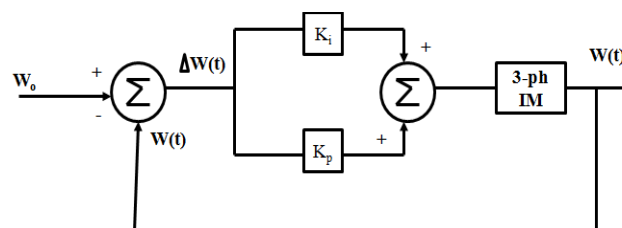


Fig. 8 Block Diagram of PI Controller.

The controller output in this case is

$$u(t) = K_p \cdot e(t) + K_i \int e(t) dt$$

Fig. 8 block diagram PI controller an integral error compensation scheme, the output response depends in some manner upon the integral of the actuating signal. This type of compensation is introduced by a using a controller which produces an output signal consisting of two terms, one proportional to the actuating signal and the other proportional to its integral. Such a controller is called proportional plus integral controller or PI controller.[20]



5.2 Controller Design

This section presents the controller design for a single-phase grid-connected PV system using the partial feedback linearization method as the system is partially linearized. Some steps need to be followed to obtain the control law through the proposed method which is discussed below:

1] Step 1: Nonlinear Coordinate Transformation and Partial Linearization:

A nonlinear coordinate transformation can be written as

$$\tilde{z} = \tilde{\mathcal{O}}(x) \quad (17)$$

where $\tilde{\mathcal{O}}$ is the function of x . For a single-phase grid-connected PV system, we choose,

$$\tilde{z}_1 = \tilde{\mathcal{O}}_1(x) = h(x) = i \quad (18)$$

Using the above transformation, the partially linearized system can be obtained as follows:

$$\dot{\tilde{z}}_1 = \frac{\partial h(x)}{\partial x} \dot{x} = L_f h(x) + L_g h(x)u \quad (19)$$

For the PV system,

$$\dot{\tilde{z}}_1 = \frac{-Ri - \varepsilon}{L} + \frac{v}{L}u \quad (20)$$

Equation (20) can be written as the following linearized form:

$$\dot{\tilde{z}}_1 = \tilde{v} \quad (21)$$

where \tilde{v} is the linear control input which can be expressed as

$$\tilde{v} = \frac{-Ri - \varepsilon}{L} + \frac{v}{L}u \quad (22)$$

and obtained using a linear control technique for system (21). But before designing and implementing controller through partial feedback linearization, it is essential to check the stability of internal dynamics of the system which is presented in the next step.

2] Step 2: Stability of Internal Dynamics of a Grid-Connected PV System:

In the previous step, the second-order PV system (8) is transformed into a first-order system (21). Lyapunov functions are the functions that are applicable to analyze the stability of the equilibrium states for dynamical systems. Lyapunov function can be defined as, "If a function $V(x)$ is positive definite and if its time derivative along any state trajectory of the system is negative definite, i.e. $\dot{V}(x) \leq 0$, then $V(x)$ is said to be a Lyapunov function". From the definition of the Lyapunov function or energy function, it can be seen that the derivative of this function is negative which means that for each state, the control law will reduce the energy V of the system. If in each state it is possible to find out a control law to reduce the energy of then system, it is possible to bring the energy of the system to zero, i.e., to bring the system to a stop which means the stable condition of the system.

From the perspective of the dynamical system stability, there exists a Lyapunov function for each dynamical system if the system is inherently stable, i.e., the internal dynamics of the system is stable. Since the main aim of the proposed controller is to track the reference current efficiently, i.e., with zero tracking error, the Lyapunov function can be constructed by considering only the current equation. In this case, the energy function for the purpose of controlling current can be written as

$$V = \frac{1}{2}Li^2 \quad (23)$$



Equation (23) is always positive and if the derivative of (23) is negative or zero, it will be a Lyapunov function.

The derivative of (23) can be written as

$$\dot{V} = Li \quad (24)$$

Substituting the value of from (8), we can write

$$\dot{V} = viu(t) - i^2 - \epsilon i \quad (25)$$

Now, using the value $u(t)$ from (22) into (25), we get

$$\dot{V} = \tilde{v}i \quad (26)$$

Since \tilde{v} is a linear control input that includes the difference between the reference current and instantaneous current, i.e., $i_{ref} - i$ and the purpose of the proposed control scheme is to make this difference as zero, thus we can write

$$\tilde{v} = 0 \quad (27)$$

and using this, (26) can be written as

$$\dot{V} = 0 \quad (28)$$

Equation (28) indicates that (23) is a Lyapunov function for the considered PV system (8) and the internal dynamic of the system is stable. Therefore, the partial feedback linearization can be used to design a current controller for a single-phase grid connected PV system, and the derivation of control law is shown in the following section.

3] Step 3: Derivation of Control Law for a Grid-Connected PV System:

From (22), the control law can be obtained as follows:

$$u = \frac{1}{v} (L\dot{V} + Ri + \epsilon) \quad (29)$$

Equation (29) is the final control law for a single-phase grid-connected PV system. At this point, the only thing which needs to be designed is the new linear control input and this can be designed by any linear controller design approach. In this paper, a PI controller is used to track the reference output. The following PI controller is considered to track the output:

$$\tilde{v} = K_p(i_{ref} - i) + K_i \int_0^1 (i_{ref} - i) dt \quad (30)$$

where K_p and K_i are the proportional and integral gain of the PI controller, respectively. Here, the gains need to be selected in such a way that the output follows the reference current to minimize the error. In this paper, the gains are set as follows:

$$K_p = 2i_{ref} \quad , \quad K_i = i_{ref}^2$$

In this case, the gains of the PI controllers depend on the reference value of the current. This reference value is calculated from the MPPT. Thus, the gain of the PI controller will be updated automatically with changes in atmospheric conditions.

VI.MPPT ALGORITHM AND CALCULATION OF REFERENCE VALUE

The MPPT technique adjusts the PV array voltage in order to extract the available maximum power under all atmospheric conditions. The MPPT uses V_{pv} and i_{pv} to detect the slope and generates P_{ref} to track the maximum

power. In this paper, an incremental conductance method is used to obtain the maximum power. At maximum power point (MPP),

$$\frac{dP_{pv}}{dv_{pv}} = 0 \quad (31)$$

Where $P_{pv} = v_{pv}i_{pv}$ and if we use this relation, then from (31)

$$\frac{\Delta i_{pv}}{\Delta v_{pv}} = -\frac{i_{pv}}{v_{pv}} \quad (32)$$

Here, $\Delta i_{pv}/\Delta v_{pv}$ is the incremental conductance and i_{pv}/v_{pv} is the instantaneous conductance. The MPP can be obtained by considering the following conditions:

1. At the MPP, $\frac{\Delta i_{pv}}{\Delta v_{pv}} = -\frac{i_{pv}}{v_{pv}}$
2. At the left of MPP, $\frac{\Delta i_{pv}}{\Delta v_{pv}} > -\frac{i_{pv}}{v_{pv}}$
3. At the right of MPP, $\frac{\Delta i_{pv}}{\Delta v_{pv}} < -\frac{i_{pv}}{v_{pv}}$

If a PV system satisfies condition 1, the voltage is ascertained at the MPP voltage and fixed at this voltage until the MPPT encounters a change due to the changes in atmospheric conditions. If the atmospheric conditions change in such a way that the PV system holds condition 2, then it is essential to increase the reference voltage to achieve the MPPT and the opposite is true for condition 3.

At the MPP, the reference output power generated by the PV system is

$$P_{ref} = v_{pv}i_{pv} \quad (33)$$

Since P_{ref} is also the maximum power which is supplied to the grid, therefore,

$$P_{Grid} = ei = V_m \sin \omega t \times I_m \sin \omega t = \frac{V_m I_m}{2} (1 - \cos 2\omega t) \quad (34)$$

where I_m is the amplitude of the injected current. The average power (P_{av}) into the grid can be written as

$$P_{av} = \frac{2}{T} \int_0^{\frac{T}{2}} \frac{V_m I_m}{2} (1 - \cos 2\omega t) dt = \frac{V_m I_m}{2} \quad (35)$$

The MPPT technique controls P_{av} to follow the reference power P_{ref} and at this stage the magnitude of the reference current I_{ref} will be I_{refm} . Therefore, the above equation can be written as

$$P_{ref} = \frac{V_m I_{refm}}{2} \quad (36)$$

Which implies that ,

$$I_{refm} = \frac{2P_{ref}}{V_m} \quad (37)$$

Finally, the reference current into the grid can be calculated as

$$i_{ref} = \frac{2P_{ref}}{V_m} \sin \omega t \quad (38)$$

And this reference current is used for the controller which can be obtained using a phase lock loop (PLL).

VII. CONTROLLER PERFORMANCE EVALUATION

First, a simple single-phase grid-connected PV system and then a PV system, similar to the practical system, are considered to evaluate the performance of the designed controller. Finally, the designed control algorithm is validated through some experimental results. The implementation block diagram of a partial feedback linearizing controller for a single-phase grid-connected PV system is shown in Fig. 9, in which it can be seen that the magnitude of the reference current for the linear controller is obtained from the MPPT and the angle is extracted from the grid current using a PLL. The controller is a combination of a linear and partial feedback linearizing controller. Finally, the control input is implemented through the inverter switches using a pulse width modulation (PWM) technique where the switching frequency of the inverter is considered as 10 kHz.

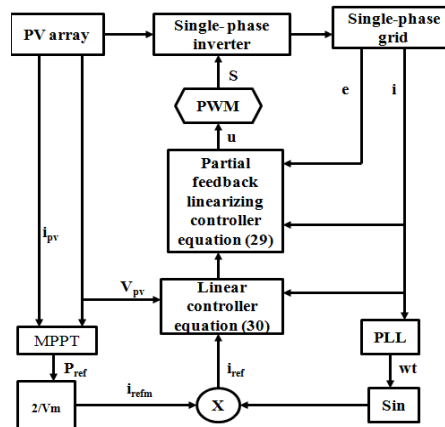


Fig. 9 Implementation Block Diagram Of Partial Feedback Linearizing Controller.

7.1. Performance Evaluation on a Simple System

In this section, the performance of the designed controller is evaluated on the simple system as shown in Fig. 9. To simulate the performance at this stage, a PV array consisting of ten PV cells, characterized by a rated current of 2.0 A, is connected in parallel. There are two bunch of PV cell, characterized by a rated voltage of 76.5 V, and connected in series. Thus, the total output voltage of the PV array is 153 V, the output current is 10 A, and the total power is 750 W. The value of the dc-link capacitor is 1000 μf . The line resistance is 0.1 Ω and the inductance is 10 mH. The grid voltage is 240V and the frequency is 50 Hz. The performance of the designed controller is evaluated under standard and changing atmospheric conditions through the following case studies.

Case 1: Controller Performance under Standard Atmospheric Conditions:

At this stage, the system is simulated under standard atmospheric condition in which the solar irradiation is considered as and the temperature as 298 K. At this condition, the output power of the PV unit from which it can be seen that there are some fluctuations due to the nonlinear characteristics of the PV system. The main purpose of the control action is that the grid current will follow the reference current when the maximum power extraction from the MPPT is 700W. This can be performed by regulating the inverter switches through the proper control scheme when the MPPT is achieved. Here comparison is shown in this nonlinear grid current (violet) and hysteresis grid current (yellow line) are shown in Fig. 14 and 15 from 0 to 0.5 s with the proposed control scheme

Case 2: Controller Performance under Changing Atmospheric Conditions:

In a practical PV system, the atmospheric condition changes continuously for which there exists variations in the cell's working temperature and solar irradiation. Due to the changes in atmospheric conditions, the output voltage, current, and power of the PV unit change significantly. For example, if a single module of a series string is partially shaded, its output current will be reduced which will indicate the operating point of the whole string. Fig. 22 and 23 shows the performance of the proposed current controller with changes in atmospheric conditions. From Fig. 20 and 21, it can be seen that the PV system operates under standard atmospheric conditions from 0. to 0.5 s. But the irradiation changes from 1000 to 700 w/sq.m at 0.2 s and the weather remains cloudy, i.e., the PV system is shaded until 0.2s to 0.35s. At this stage, the amount of power delivered to the grid will be changed and the MPPT will select a different MPP, but the grid voltage will be the same. The change in the grid current is also shown in Fig. 22 and 23. After 0.35 s, with the proposed controller, the non linear current controller grid current (violet line) is similar to its previous value as the system again operates at standard atmospheric conditions, but the hysteresis current controller (yellow line) is not capable to track the reference current accurately.

Case 3: Controller Performance During Fault:

A line-to-ground fault is considered at an instance at the terminal of PV unit to evaluate the performance of the proposed current controller. When such faults are applied, PV units will not supply any power into the grid and load. Under this case study, the performance of the proposed controller is shown in Fig. 17 and 18 from where it can be seen that the PV unit is not injecting any current into the grid from 0.25 to 0.35 s as the fault is applied for this period. In this case study, the pre-fault and post-fault conditions are considered as standard atmospheric conditions. The proposed controller maintains the post-fault steady state as soon as the fault is cleared but with the hysteresis controller the system becomes unstable. The simulation results show the superiority of the proposed control scheme.

7.2 Simulation Models & results

7.2.1 At Standard Atmospheric Condition

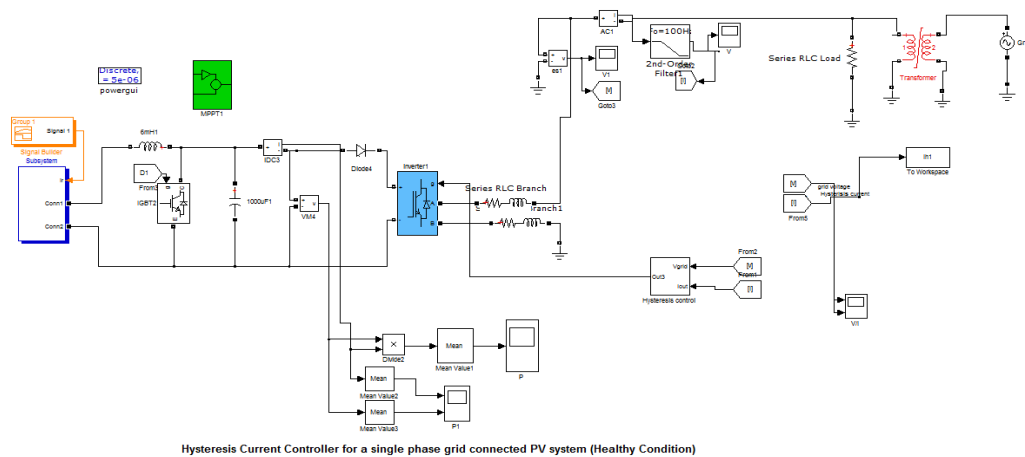


Fig. 10 Hysteresis Controller Simulation Model at Standard Atmospheric Condition

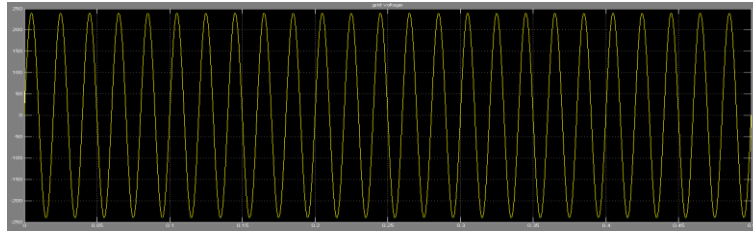


Fig. 11 Hysteresis and Nonlinear current controller grid voltage at standard atmospheric condition

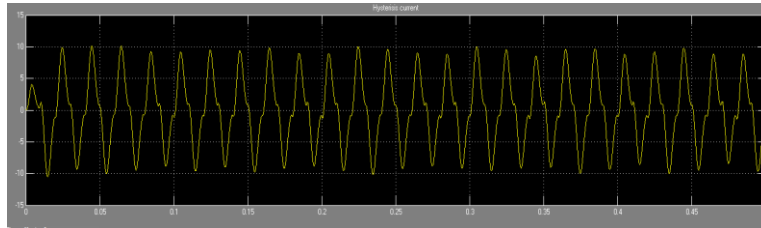


Fig. 12 hysteresis current at standard atmospheric condition



Fig. 13 Nonlinear current at standard atmospheric condition

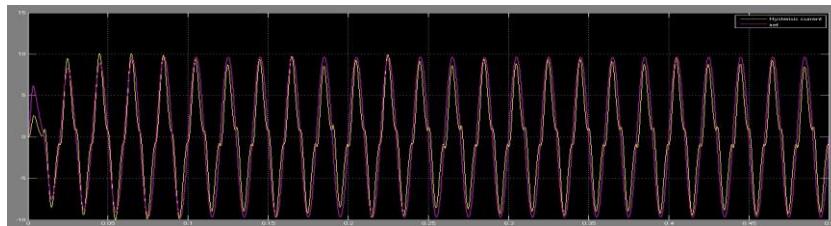


Fig. 14 current comparison of hysteresis current and reference current at standard atmospheric condition

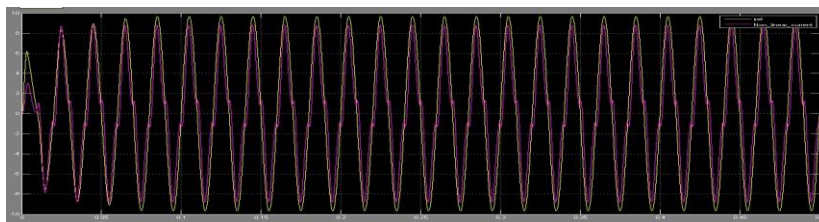


Fig. 15 current comparison of Nonlinear current and reference current at standard atmospheric condition

7.2.2. Under fault Condition:-

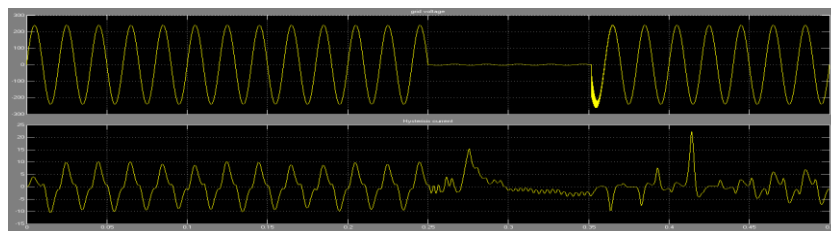


Fig. 16 Hysteresis Current Controller Voltage And Current During Fault Condition

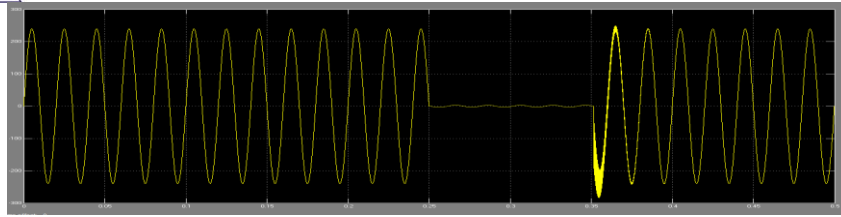


Fig. 17 Non Linear Current Controller Voltage During Fault Condition

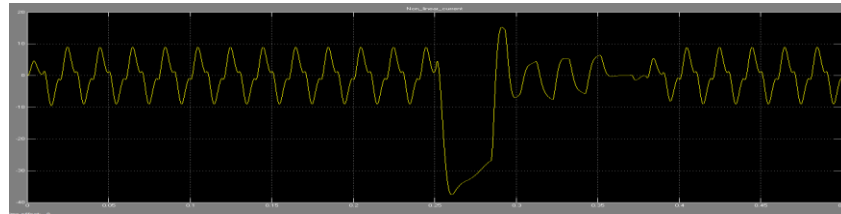


Fig. 18 Non Linear current controller current during fault condition

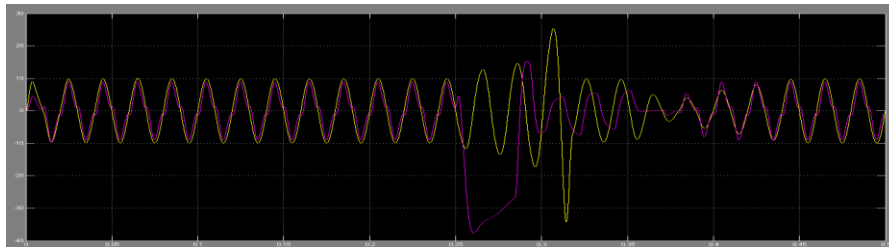


Fig. 19 Current Comparison of Hysteresis and Non Linear current controller during fault condition

7.2.3. changing atmospheric condition

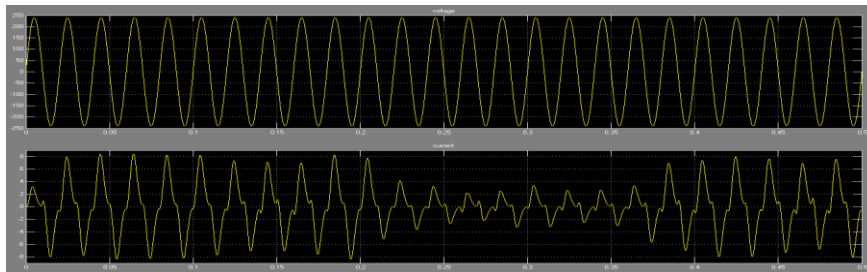


Fig. 20 Hysteresis Current Controller Voltage And Current At Changing Atmospheric Condition

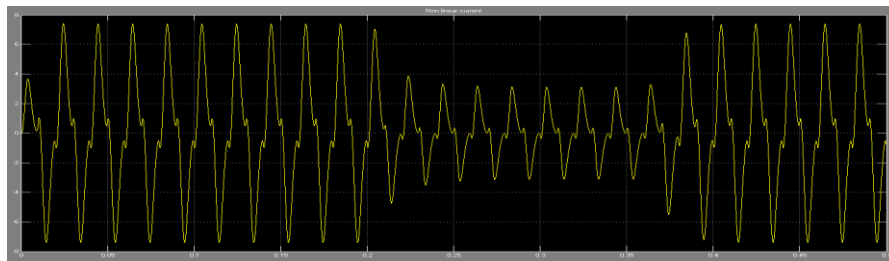


Fig. 21 Non Linear Current Controller Current At Changing Atmospheric Condition

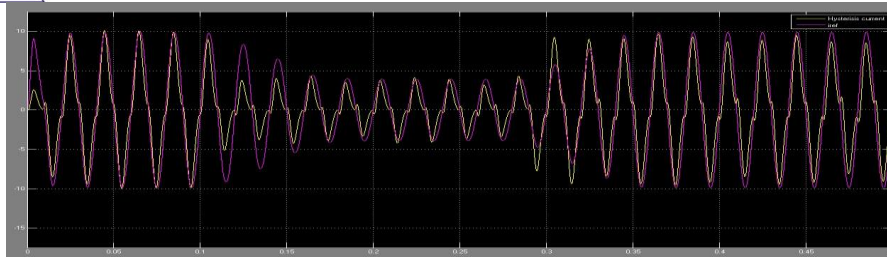


Fig. 22 Comparison Of Hysteresis Current And Reference Current At Change In Atmospheric Condition

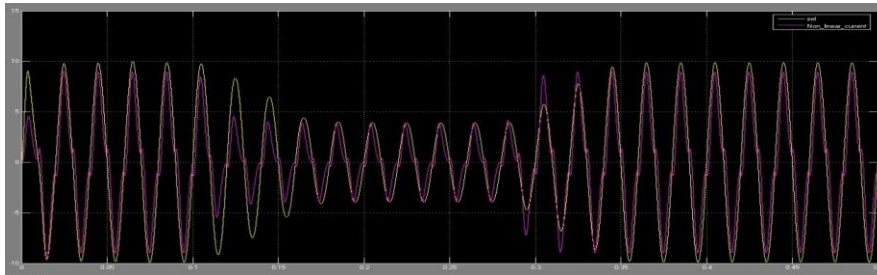


Fig. 23 Comparison Of Nonlinear Current And Reference Current At Change In Atmospheric Condition

VII. CONCLUSION

A partial feedback linearizing nonlinear current control scheme was presented to improve the dynamic performance of a single-phase grid-connected PV system with changes in atmospheric conditions, variations in load conditions, and faults on different parts of the system. All the possible nonlinearities are very well canceled by the proposed controller designed approach by transforming the PV system into a reduced order linear system with stable internal dynamics. The injected current into grid is controlled to ensure the operation of the PV system at the MPP. Future work will deal with the extension of the proposed method by considering some mismatches within the PV model and implementation on a laboratory-based system. A review on various current control techniques/schemes has been discussed here & it is found that nonlinear current control scheme, presented & validated using MATLAB simulation is more efficient compared to hysteresis current control. This work is supported with results obtained in MATLAB simulation through waveforms.

VIII. ACKNOWLEDGEMENT

I would like to express my deepest sense of gratitude to my guide Prof. A. D. Matre who offered his continuous advice and encouragement throughout the course of this seminar. I thank him for the systematic guidance and great effort he put into training me in the scientific field.

I am thankful to Prof. D. M. Sonje- PG Coordinator, Electrical Engineering Department, Prof. M.K. Chaudhari - Head of Electrical Engineering Department, Dr. P. C. Kulkarni Principal, GES- RHSCOE, Nasik for the support and encouragement whenever I was in need.

I am thankful to all faculty members of GES-RHSCOE, Nasik, my colleagues & my parents for their valuable time, support and encouragement. **Ms. Ashwini Ashok Pakhale**



REFERENCES

- [1] M. A. Mahmud, H. R. Pota, and M. J. Hossain, "Nonlinear Current Control Scheme for a Single-Phase Grid-Connected Photovoltaic System" IEEE TRANSACTIONS ON SUSTAINABLE ENERGY, VOL. 5, NO. 1, JANUARY 2014
- [2] T. Kato, T. Inoue, and Y. Suzuoki, "Impact of Large-scale Penetration of Photovoltaic Power Generation Systems on Fluctuation Property of Electricity Load" 2010
- [3] I. Houssamo, F. Locment, and M. Sechilariu, "Maximum power point tracking for photovoltaic power system: Development and experimental comparison of two algorithms," Renew. Energy, vol. 35, no. 10, pp. 2381–2387, Oct. 2010
- [4] D. Casadei, G. Grandi, and C. Rossi, "Single-phase single-stage photovoltaic generation system based on a ripple correlation control maximum power point tracking," IEEE Trans. Energy Convers., vol. 21, no. 2, pp. 562–568, Jun. 2006
- [5] Sreekanth G, Narender Reddy N, Durga Prasad A, Nagendrababu V " A Mppt Algorithm Based Pv System Connected To Single Phase Voltage Controlled Grid" International Journal of Advancements in Research & Technology, Volume 1, Issue 5, October-2012 1 ISSN 2278-7763
- [6] T. Esumi and P. L. Chapman, "Comparison of photovoltaic array maximum power point tracking techniques," IEEE Trans. Energy Convers., vol. 22, no. 2, pp. 439–449, Jun. 2007.
- [7] M. E. Ropp and S. Gonzalez, "Development of a MATLAB/Simulink model of a single-phase grid-connected photovoltaic system," IEEE Trans. Energy Convers., vol. 24, no. 1, pp. 195–202, Mar. 2009.
- [8] B. D. Subudhi and R. Pradhan, "A comparative study on maximum power point tracking techniques for photovoltaic power systems," IEEE Trans. Sustain. Energy, vol. 4, no. 1, pp. 89–98, Jan. 2013.
- [9] Mattia Ricco, Patrizio Manganiello, Eric Monmasson, Giovanni Petrone, and Giovanni Spagnuolo, "FPGA-Based Implementation of Dual Kalman Filter for PV MPPT Applications" IEEE Transactions On Industrial Informatics, 2015.
- [10] J. Selvaraj and N. A. Rahim, "Multilevel inverter for grid-connected PV system employing digital PI controller," IEEE Trans. Ind. Electron., vol. 56, no. 1, pp. 149–158, Jan. 2009.
- [11] P. P. Dash and M. Kazerani, "Dynamic modeling and performance analysis of a grid-connected current-source inverter-based photovoltaic system," IEEE Trans. Sustain. Energy, vol. 2, no. 4, pp. 443–450, Oct. 2011
- [12] N. A. Rahim, J. Selvaraj, and C. C. Krismadinata, "Hysteresis current control and sensorless MPPT for grid-connected photovoltaic systems," in Proc. IEEE Int. Symp. Industrial Electronics, Vigo, Spain, 2007, pp. 572–577.
- [13] A. Kotsopoulos, J. L. Duarte, and M. A. M. Hendrix, "A predictive control scheme for DC voltage and AC current in grid-connected photovoltaic inverters with minimum DC link capacitance," in Proc. 27th Annu. Conf. IEEE Industrial Electronics Society, Colorado, USA, 2001, pp. 1994–1999.
- [14] E. Bianconi, J. Calvente, R. Giral, E. Mamarelis, G. Petrone, A. Ramos-Paja, G. Spagnuolo, and M. Vitelli, "A fast current-based MPPT technique employing sliding mode control," IEEE Trans. Ind. Electron., vol. 60, no. 3, pp. 1168–1178, Mar. 2013



- [15] T. L. Nguyen and K.-S. Low, "A global maximum power point tracking scheme employing DIRECT search algorithm for photovoltaic systems," IEEE Trans. Ind. Electron., vol. 57, no. 10, pp. 3456–3467, Oct. 2010
- [16] Arun Raj, Anu Gopinath " Proportional plus Integral (PI) Control for Maximum Power Point Tracking in Photovoltaic Systems" International Research Journal of Engineering and Technology (IRJET) Volume: 02 Issue: 06 | Sep-2015
- [17] Florida solar energy centre www.fsec.ucf.edu
- [18] Miro Zeman Delft University of Technology "PHOTOVOLTAIC SYSTEMS," ocw.tudelft.nl/fileadmin/ocw/courses, CH9-Photovoltaic_systems.pdf.
- [19] Aurel Botezan, Ioan Vadan and Silviu stefanescu "Hysteresis Current Control of the Single – Phase Active Filter" Annals of university of Craiova ,Electrical Engineering series, No 37,2013,ISSN 1842-4805
- [20] K Smriti Rao, Ravi Mishra " Comparative study of P, PI and PID controller for speed control of VSI-fed induction motor" 2014 IJEDR | Volume 2, Issue 2 | ISSN: 2321-9939.